Finite Element Simulation on the Tensile Property of Steel Cord at Different Lay Lengths Under Axial Loading

Shanling Han[1], Lingkang Kong[1], Yanmeng Chi[1], Long Chen[2] and Yong Li[1*]
[1]*College of Mechanical and Electronic Engineering, Shandong University of Science and Technology, Qingdao, Shandong, China*
[2]*College of Materials Science and Engineering, Shandong University of Science and Technology, Qingdao, Shandong, China*

Keywords: Steel Cord, Lay Length, Tensile Property, Finite Element Analysis, Axial Loading.

Abstract: Steel cord is the primary load-bearing component of a tire, and as the tire environment becomes more complicated and variable, greater tensile property demands are placed on the cord. There are several factors that affect the tensile property of steel cord, with lay length being an important factor that is closely related to the durability and quality of steel cord. Therefore, this paper takes 3×0.20+6×0.35HT steel cord as the research object, establishes the parametric model with varying lay lengths, and employs the finite element method to examine the effect of varying lay lengths on the tensile property. The results indicate that the breaking strain of steel cord is lowest at the standard lay length. Furthermore, the breaking strain of steel cord increases regardless of whether the lay length of the inner and outer monofilaments increases or decreases. This study provides a basis and reference for the optimal design and manufacture of steel cord.

1 INTRODUCTION

Steel cord is widely used in rubber products (Zhang, 2019) such as tires and transportation belts because of its high tensile strength, malleability, and stability (Prawoto, 2012). The load-bearing capacity and service life of steel cord are crucial to the safe operation of rubber products. As the primary skeleton material of rubber products, steel cord is subjected to loads such as tension (Gurevich, 2022) and impact (Li, 2021), and its load-bearing strength and safe operation are crucial to the service life (Kruzel, 2019). During use, the steel cord will be abrasive and loose between the monofilaments; as a result, the failure of the steel cord due to stretching has become a major concern among engineering designers and end-users. To improve the safety factor of steel cord, the lay length must be investigated. Nonetheless, in the development of steel cord, the steel cord must be repeatedly tested to determine its optimal parameters, which is poorly oriented, time-consuming, and wasteful of resources. For analyzing the stress-strain analysis of complex metal structural products, finite element analysis is more intuitive, highly accurate, and widely used in the industry (Korunović, 2019). Numerous scholars have conducted extensive research on this topic, concentrating primarily on the axial tensile property of steel cord.

Stanova (Stanova, 2011; Stanova, 2011) developed mathematical geometric models of single and double-layered wire ropes with specified initial parameters, discussed the application of the derived mathematical models, and carried out numerical simulations of the established finite element models for multilateral strands subjected to tension tests. Chen (Chen,2021) and Abdullah (Abdullah, 2016) have proposed techniques for modeling that are more refined. Extensive research has been conducted on the stress distribution law of the wire during tensioning of the locking coil wire rope, as well as the behavior of the prestressed strand after stress and fracture. Fedorko (Fedorko, 2014) proposed a criterion for the failure of locking coil wire ropes. And proposed an accurate computational three-dimensional solid modeling method for two-layer triangular wire strands for finite element analysis, and used the three-dimensional computational model for finite element analysis of two-layer triangular steel strands subjected to tensile loads. Ma (Ma, 2022) simulated the multi-pass tensile process of wire with and without eccentric inclusion under different back tensions using the finite element method. All previous finite element analyses made use of steel cord with a standard lay length, ignoring the effect of lay length

Han, S., Kong, L., Chi, Y., Chen, L. and Li, Y.
Finite Element Simulation on The Tensile Property of Steel Cord at Different Lay Lengths Under Axial Loading.
DOI: 10.5220/0012149500003562
In *Proceedings of the 1st International Conference on Data Processing, Control and Simulation (ICDPCS 2023)*, pages 64-71
ISBN: 978-989-758-675-0

on the tensile property of the steel cord. In general, the breaking strain decreases as the lay length increases. 3 × 4 × 0.22HE compared with 3 + 9 × 0.22HE, the former lay length (3.15S/6.3S) than the latter lay length (6.3S/12.5S) is twice as small, although the diameter of the two monofilament and the number of filaments is the same, but the former break strain of up to 5-10%, the latter only about 2%; from the physical test data, the former break tension of 912 N, the latter is 830 N. the strength twist loss of high elongation cord is often above 20%. Therefore, the influence of lay length on tensile property needs to be further explored.

This paper first will obtain the tensile curve of 3×0.20+6×0.35HT using a tensile machine, then will establish the parametric model of 3×0.20+6×0.35HT and verify the accuracy and feasibility of the simulation by comparing it with experimental data. Finally, models with an inner lay length of 10 mm and an outer lay length of 12.5, 14.0, 16.0, 18.0, 20.0, and 22.4 mm will be created, as well as models with an inner lay length of 8.0, 9.0, 10.0, 11.2, 12.5 and 14.0 mm and an outer lay length of 18 mm. To examine the effect of different lay lengths on tensile property.

2 FINITE ELEMENT ANALYSIS OF TENSILE STEEL CORD

2.1 The Establishment of the Finite Element Model

As an example, this study models a steel cord of type 3×0.20+6×0.35HT (Fig. 1a). The cross-sectional view of this cord is shown in Fig. 1(b). This type of cord is one of the simpler cord structures, consisting of two layers of steel monofilaments twisted inside and outside, with each layer evenly distributed along the circumference and both layers in a single spiral structure. The parameters such as diameter, lay length, diameter, distance from inner and outer cord to the center are listed in Table 1.

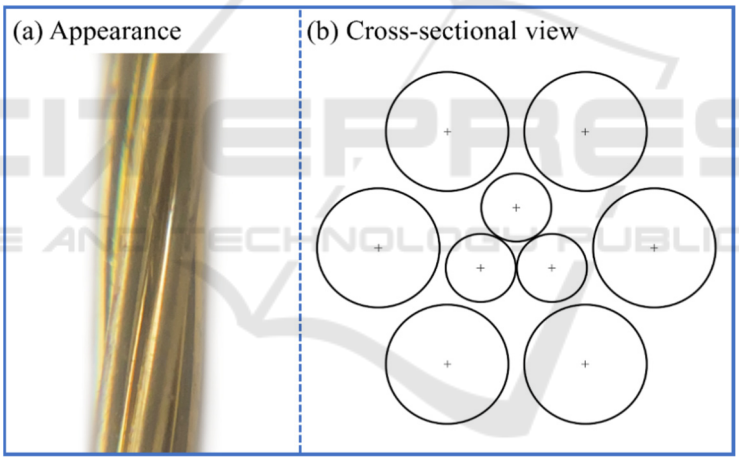

Figure 1: Steel cord: (a) appearance, (b) cross-sectional view.

Table 1: 3×0.20+6×0.35HT steel cord parameters.

Material properties	Value
Length (mm)	15
Diameter (mm)	1.13
Inner cord lay length (mm)	10
Outer cord lay length (mm)	18
Inner cord diameter (mm)	0.2
Outer cord diameter (mm)	0.35
The distance from the inner cord to the center (mm)	0.118
The distance from the outer cord to the center (mm)	0.394
Breaking stress (MPa)	2918.68
Breaking strain (%)	0.0208

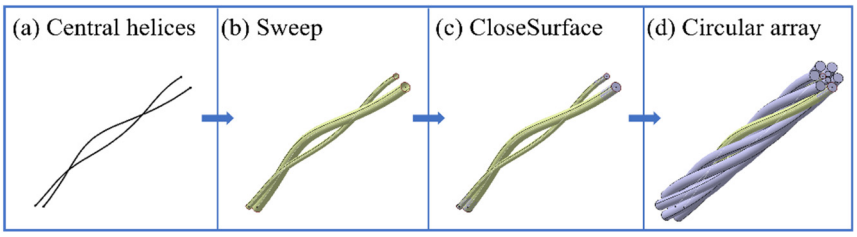

Figure 2: Specific procedure: (a) generates center helices, (b) sweep, (c) closed, (d) circular array.

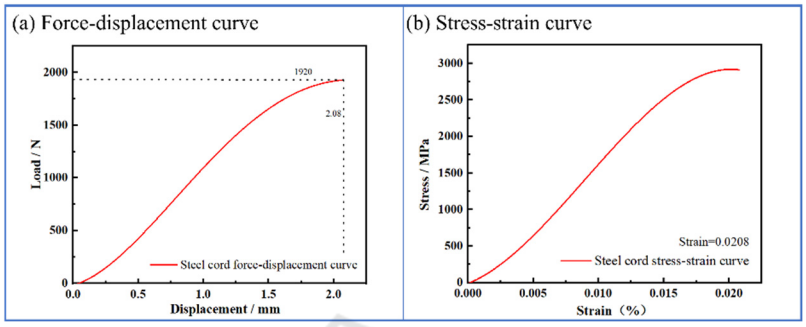

Figure 3: 3×0.20+6×0.35HT steel cord: (a) force- displacement curve, (b) stress-strain curve.

The standard lay lengths are 2.5, 2.8, 3.1, 3.5, 4.0, 4.5, 5.0, 5.6, 6.3, 7.1, 8.0, 9.0, 10.0, 11.2, 12.5, 14.0, 16.0, 18.0, 20.0, 22.4, 25.0, etc. 3×0.20+6×0.35HT is used as the research object, and models with inner lay length of 10 mm and an outer lay length of 12.5, 14.0, 16.0, 18.0, 20.0, and 22.4 mm are established, as well as models with inner lay lengths of 8.0, 9.0, 10.0, 11.2, 12.5, and 14.0 mm and outer lay lengths of 18 mm. These models are used to examine the effect of different lay lengths on the stress distribution and strain.

Based on the above parameters, parametric modeling of the steel cord can be achieved by the spiral sweep and circular array functions. Firstly, the center line of the steel cord and the cross section of two kinds of monofilaments are established (Fig. 2a), then the helices are generated, and the curve smoothing is used to adjust the curvature inconsistency of the intersection point of the helix, then the solid model of the monofilaments is completed with the sweep (Fig. 2b) and closed surface (Fig. 2c) commands, and finally the complete steel cord is completed with the circular array (Fig. 2d) command.

2.2 Material Properties

Analysis of steel cord using finite elements is a nonlinear problem requiring the definition of material parameters, the construction of the mesh system, the configuration of the solver, the construction of connection relations, the establishment of boundary conditions, and post-processing. Based on the explicit dynamic solver, a simulation study of the tensile steel cord is carried out

The steel cord is a high-carbon steel, and the steel cord is an elastoplastic material. In material systems, elastoplastic materials are usually defined by the following parameters: ductile damage, density, elasticity, and plasticity. To simulate a real cord stretching experiment, the steel cord is pulled off by the traditional German Zwick electronic universal testing machine with a tensile speed of 100 mm/min. The stress-strain curve is calculated from the force-displacement curve of the cord stretched in the press, and the curve is measured and plotted using specialized tools. these parameters are calculated from the stress-strain curve (Fig. 3a) obtained by stretching 3×0.20+6×0.35HT cord in a press, and the stress-strain curve is shown in Fig. 3(b).

The density of steel cord is $7.95\times10^{-9}\,t/mm^3$; Young's modulus of elastic property is $1.81\times10^{11}\,N/mm^2$, Poisson's ratio is 0.3; breaking strain, stress triaxiality, strain ratio and damage evolution of ductile damage are 0.207, 0.333, 0.001 and 0.02 respectively. The experimental data of the press are given in terms of nominal stress and nominal strain and considering the effect of material necking on the data. The real stress and real strain are used to define the plasticity data. Therefore, the transformation from nominal stress/strain to real stress/strain has to be realized, and the transformed stress-strain curve is shown in Fig. 3.

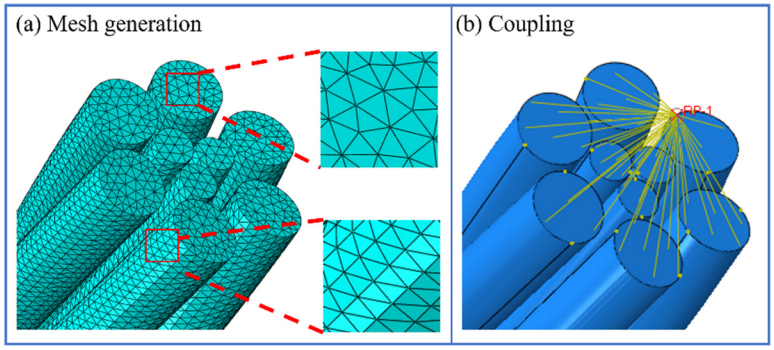

Figure 4: Key steps of finite element analysis: (a) mesh generation, (b) coupling.

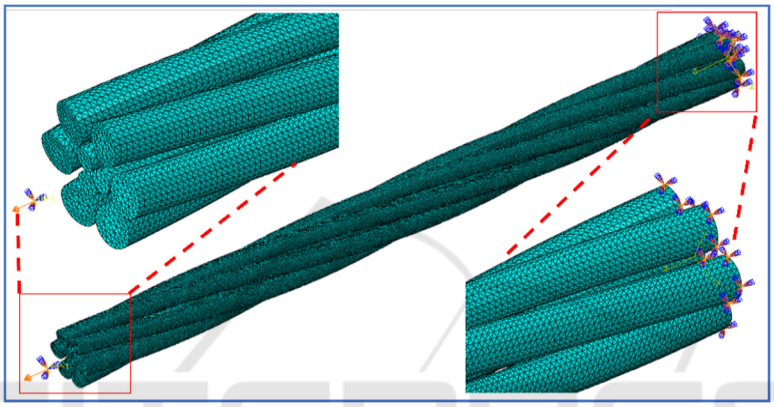

Figure 5: Boundary conditions at both ends of the steel cord.

2.3 Mesh Generation and Contact Condition

Because each monofilament within the steel cord has central symmetry, the mesh division of each monofilament also has central symmetry. In consideration of the geometric characteristics of the monofilament and contact, etc., and to eliminate the influence of the mesh type on the analysis of experimental results, the uniform use of C3D4 mesh type, and to consider the accuracy of simulation results and calculation time. Meshes with dimensions of 0.05 mm are used for the finite element analysis. The meshed model can be seen in Fig. 4(a).

Considering the contact between the monofilaments of the steel cord during the tensile process, the surface-to-surface contact type is defined. This method yields more accurate results, but it is time-consuming. Therefore, instead of setting up contact pairs for two individual monofilaments, a global setup is used with a contact behavior of hard contact normal to the steel cord surface and a friction coefficient of 0.19 between brasses of the steel cord surface material in the radial direction.

To accurately simulate the tensile experiment on both ends of the steel cord testing machine's stretching state, the simulation incorporated the following boundary conditions: one end of the steel cord degrees of freedom by way of motion coupling constraint to the reference point RP-1 (Fig. 4b). the reference point RP-1 coupling steel cord end surface into a fixed relationship, the reference point has six degrees of freedom, specifically three translational degrees of freedom, three rotational degrees of freedom. The load is only applied in the axial direction to the monofilament, and the remaining degrees of freedom are null.

2.4 Boundary Conditions

The boundary conditions of the steel cord are imposed as shown in Fig. 5, where the reference point RP-1 moves uniformly along the axial direction at 0.6 mm in 0.15 s under axial tension, and the other end of the steel cord is fixedly restrained.

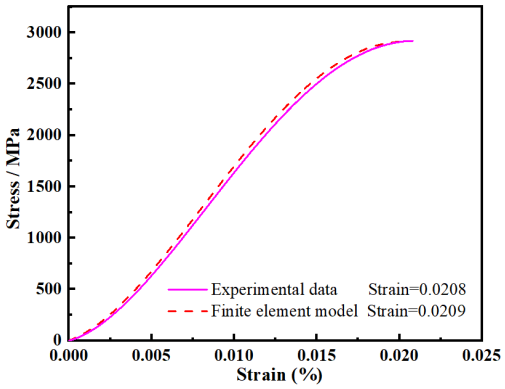

Figure 6: Experimental data and finite element model of tensile stress-strain curves.

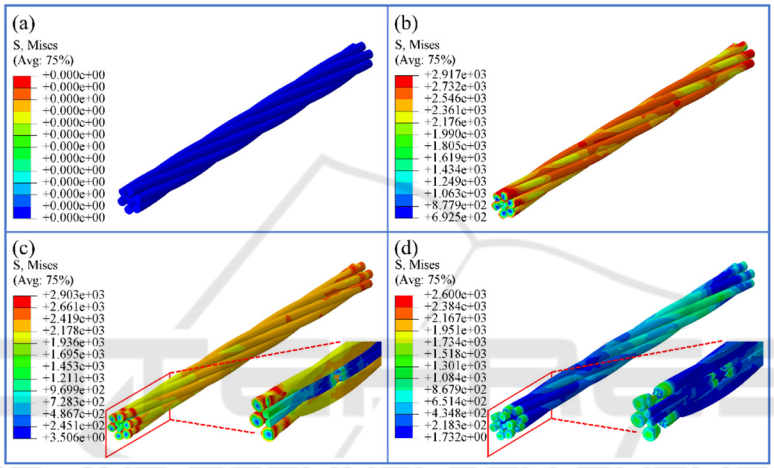

Figure 7: Tensile process of steel cord: (a) initial state, (b) maximum stress reached, (c) inner layer monofilament breakage, (d) outer layer monofilament breakage.

3 RESULTS AND DISCUSSION

Two types of results to study the overall mechanical property of the tensile action steel cord are analyzed in this article: stress distribution and strain.

(1) First, the tensile simulation is conducted for the finite element model with the standard inner lay length of 10 mm and outer lay length of 18 mm, and the stress-strain curve obtained is shown in Fig. 6.

(2) The finite element model tensile process and the stresses in its cross section are shown in Fig. 7 and Fig. 8. The stresses within the steel cord cross section exhibit a centrally symmetrical distribution and a decreasing trend outward. Compared to the outer layer, the inner layer of the cord is subjected to a greater stress, which means that the inner monofilament is subjected to a larger load. As a result, inner monofilament breaks first (Fig. 7c), followed by the outer monofilament (Fig. 7d). Due to the different

The breaking strain is 2.09%, and the deviation from the tensile test is only 0.625%; the tensile property of the steel cord obtained from the simulation result are consistent with the actual measured value, which provides a comparison of the tensile property of the steel cord. This provides a basis for the tensile comparison of finite element models with different lay lengths, and the finite element analysis process is also authentic and reliable.

lay lengths of the steel cord, the cross section of the steel cord is roughly divided into three cases from a radial perspective: first (Fig. 8b1), there is a small gap between the monofilaments of the steel cord, relatively independent, there is no extrusion phenomenon, the steel cord is only subject to axial tensile load, when the load distribution is relatively uniform and no stress concentration phenomenon arises. Second (Fig. 8b2), the inner three monofilaments are extruded by the outer six

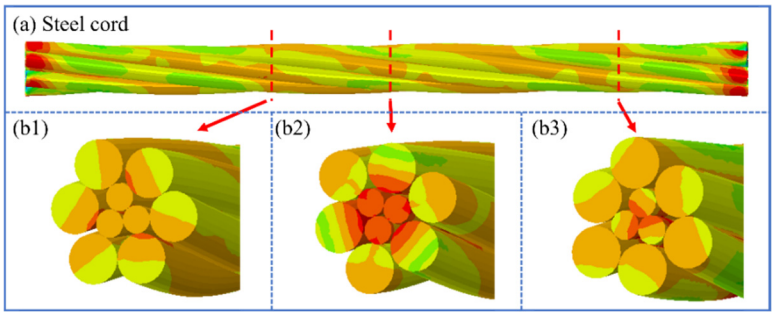

Figure 8: Stress distribution: (a) steel cord in the stretched state, (b) three typical cross-sections.

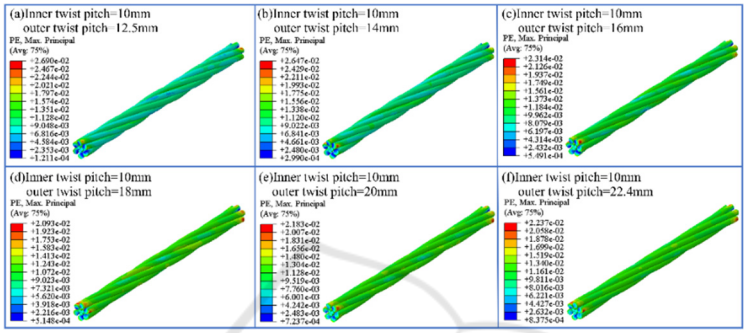

Figure 9: Steel cords with inner lay lengths of 10 mm and outer lay lengths of (a) 12.5, (b) 14.0, (c) 16.0, (d) 18.0, (e) 20.0, and (f) 22.4 mm.

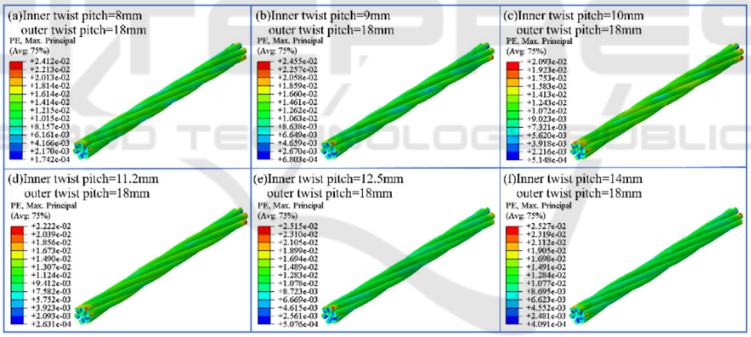

Figure 10: Steel cords with inner lay lengths of (a) 8.0, (b) 9.0, (c) 10.0, (d) 11.2, (e) 12.5, and (f) 14.0 mm and outer lay lengths of 18 mm.

monofilaments, and the inner three monofilaments are extruded from one another. When the inner monofilaments are subjected to axial tensile and extrusion, the stress is the highest; therefore, it is also easy to break in this section. Third (Fig. 8b3), the inner three monofilaments don't receive the extrusion of the outer layer of steel cord; only the inner three monofilaments extrude each other. At this group, the steel cord received tensile and extrusion force, and the stress is higher.

(3) The breaking strains at 2918 MPa for models with inner lay lengths of 10 mm and outer lay lengths of 12.5, 14.0, 16.0, 18.0, 20.0, and 22.4 mm and for models with inner lay lengths of 8.0, 9.0, 10.0, 11.2, 12.5, and 14.0 mm and outer lay lengths of 18 mm are depicted in Fig. 9 and Fig. 10. When the inner layer lay length is 10 mm and the outer layer lay length is 12.5 mm, the maximum breaking strain is 2.69%, with a deviation of 28.71% from the breaking strain of steel cord at the standard lay length. The breaking strain tends to decrease with increasing lay length for both the inner and outer layers. The minimum breaking strain for 3×0.20+6×0.35HT with standard lay lengths of 10 mm for the inner layer and 18 mm for the outer layer is 2.09%, while the breaking strain increases with increasing lay length when the inner layer lay length is greater than 10 mm and the outer layer lay length is greater than 18 mm. As shown in

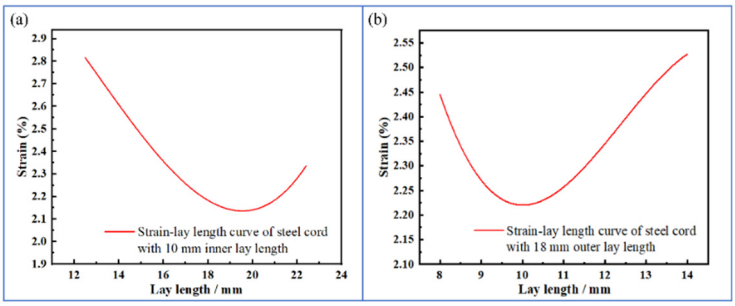

Figure 11: Strain-lay length curves: (a)steel cord with 10 mm inner lay length, (b) steel cord with 18 mm outer lay length.

Fig. 11, it can be observed that the breaking strain of the steel cord increase regardless of whether the lay length is increased or decreased in comparison to the standard lay length, which is consistent with the results of actual steel cord manufacture.

4 CONCLUSION

Steel cord tensile property are influenced by several parameters, including lay length. A parametric model of 3×0.20+6×0.35HT steel cord is developed and compared to the stress-strain curve obtained from a tensile test. The deviation of the breaking strain from the tensile test is only 0.625%, which proves the simulation's accuracy and prepares for the upcoming experiments.

In this paper, the steel cord loading cross-section is categorized based on the difference in stress distribution: first, each monofilament of the inner and outer layers is extrusion-free and only experiences tensile stress. Second, the inner monofilaments extrude each other and receive the extruding effect of the six outer monofilaments simultaneously, at which group the inner monofilaments carry the most stress and will break first, followed by the outer monofilaments. Third, just the inner monofilaments extrude each other while the outer monofilaments do not exert any pressure. This research also compares the breaking strain of steel cords with various lay lengths and standard lay lengths. When the lay length is standard, the steel cord's breaking strain is minimal. Whether the lay length of the inner or outer monofilaments increases or decreases, the steel cord fracture strain increases. Also consistent with actual steel cord manufacturing results.

ACKNOWLEDGMENT

This work was supported by National Nature Science Foundation of Shandong Province of China (Grant No. ZR2022ME118).

CONFLICTS OF INTEREST

The authors declare that they have no known competing financial interests or personal relationships that could have appeared to influence the work reported in this paper.

REFERENCES

Zhang P, Duan M, Ma J, zhang Y. (2019). A precise mathematical model for geometric modeling of wire rope strands structure. *Applied Mathematical Modelling*. *76*:151-71.

Prawoto Y, Mazlan RB. (2012). Wire ropes: Computational, mechanical, and metallurgical properties under tension loading. *Computational Materials Science*. *56*:174-8.

Gurevich L, Danenko V, Bogdanov A, Kulevich V. (2022). Analysis of the stress-strain state of steel closed ropes under tension and torsion. *International Journal of Advanced Manufacturing Technology*. *118*:15-22.

Li Y, Sun X, Song J, Zhang S, Han S. (2021). Topological structure and experimental investigation of a novel whole tire bead. *Materials & Design*. *203*:109592.

Kruzel R, Ulewicz M. (2019). The fatigue strength of bidirectionally bent steel cord used in tyres. *Engineering Failure Analysis*. *105*:176-81.

Korunović N, Fragassa C, Marinković D, Vitković N, Trajanović M. (2019). Performance evaluation of cord material models applied to structural analysis of tires. *Composite Structures*. *224*:111006.

Stanova E, Fedorko G, Fabian M, Kmet S. (2011). Computer modelling of wire strands and ropes Part I: Theory and computer implementation. *Advances in*

Engineering Software. *42*:305-15.
Stanova E, Fedorko G, Fabian M, Kmet S. (2011). Computer modelling of wire strands and ropes part II: Finite element-based applications. *Advances in Engineering Software*. *42*:322-31.
Chen Z, Guo L, Liu H, Chen H. (2021). Finite element study of behaviour and interface force conditions of locked coil wire rope under axial loading. *Construction and Building Materials*. *272*:121961.
Abdullah ABM, Rice JA, Hamilton HR, Consolazio GR. (2016). An investigation on stressing and breakage response of a prestressing strand using an efficient finite element model. *Engineering Structures*. *123*:213-24.
Fedorko G, Stanova E, Molnar V, Husakova N, Kmet S. (2014). Computer modelling and finite element analysis of spiral triangular strands. *Advances in Engineering Software*. *73*:11-21.
Ma A, Zhang Y, Dong L, Yan H, Fang F, Li Z. (2022). Damage and fracture analyses of wire with off-center inclusion on multi-pass drawing under different back tensions. *Engineering Failure Analysis*. *139*:106512.